Philosophical Magazine A
Publication details, including instructions for authors and subscription information:
http://www.informaworld.com/smpp/title~content=t713396797

Interfacial microstructures of rf-sputtered TiNi shape memory alloy thin films on (100) silicon

S. K. Wu [a]; J. Z. Chen [ab]; Y. J. Wu [a]; J. Y. Wang [c]; M. N. Yu [d]; F. R. Chen [d]; J. J. Kai [d]
[a] Institute of Materials Science and Engineering, National Taiwan University, Taipei, Taiwan [b] Department of Electrical Engineering, Princeton University, New Jersey, USA [c] Materials Research and Development Center, Chung-Shan Institute of Science and Technology, Taiwan [d] Department of Engineering and System Science, National Tsing Hua University, Hsinchu, Taiwan

Online Publication Date: 01 August 2001

To cite this Article Wu, S. K., Chen, J. Z., Wu, Y. J., Wang, J. Y., Yu, M. N., Chen, F. R. and Kai, J. J.(2001)'Interfacial microstructures of rf-sputtered TiNi shape memory alloy thin films on (100) silicon',Philosophical Magazine A,81:8,1939 — 1949
To link to this Article: DOI: 10.1080/01418610108216645
URL: http://dx.doi.org/10.1080/01418610108216645

PHILOSOPHICAL MAGAZINE A, 2001, VOL. 81, NO. 8, 1939–1949

Interfacial microstructures of rf-sputtered TiNi shape memory alloy thin films on (100) silicon

S. K. WU†, J. Z. CHEN‡, Y. J. WU

Institute of Materials Science and Engineering, National Taiwan University, Taipei 106, Taiwan

J. Y. WANG

Materials Research and Development Center, Chung-Shan Institute of Science and Technology, Lung-Tan 325, Taiwan

M. N. YU, F. R. CHEN and J. J. KAI

Department of Engineering and System Science, National Tsing Hua University, Hsinchu 300, Taiwan

[*Received 19 July 2000 and accepted in revised form 20 October 2000*]

ABSTRACT

Interfacial microstructures of TiNi thin films rf sputtered on to Si(100) and post-annealed at 400–700°C for 30 mins have been investigated using analytical and high-resolution transmission electron microscopy. For annealing temperatures below 600°C, a very thin amorphous (Si, O)-rich layer is observed at the interface. Ni atoms are the primary diffusing species and $NiSi_2$ forms triangularly and epitaxially towards the Si substrate. TiNi films initially crystallize after 30 min at 500°C. Si and Ti atoms begin to migrate in specimens annealed at 600°C for 30 min. At this temperature, a near-$Ti_4Ni_4Si_7$ phase in triangular $NiSi_2$ and a near-TiNiSi phase in the TiNi film are simultaneously nucleated and grown at the interface. For the specimens annealed at 700°C for 30 min, two layers of $Ti_4Ni_4Si_7$ and TiNiSi form at the interface with the sequence TiNi/TiNiSi/$Ti_4Ni_4Si_7$/Si. Triangular $NiSi_2$ islands are now embedded in the $Ti_4Ni_4Si_7$ layer. A mechanism of interfacial microstructure evolution is proposed to explain the temperature effect on the interfacial reaction layers between the TiNi film and the Si(100).

§1. INTRODUCTION

Among many high-performance materials applied in a microactuator, TiNi thin films exhibit the significant advantages of large deformation and recovery forces (Walker *et al.* 1990, Wolf and Heuer 1995, Quandt *et al.* 1996, Krulevitch *et al.*

† Author for correspondence. Email: skw@ccms.ntu.edu.tw.

‡ Present address: Department of Electrical Engineering, Princeton University, New Jersey 08544, USA.

Philosophical Magazine A ISSN 0141–8610 print/ISSN 1460-6992 online © 2001 Taylor & Francis Ltd
http://www.tandf.co.uk/journals
DOI: 10.1080/01418610010019134

1996); thus many efforts have been made to sputter good-quality TiNi thin films (Gisser *et al.* 1992, Ishida *et al.* 1993, 1996, 1997, Chen and Wu 1999, Wu *et al.* 2000). During the fabrication processes, the interfacial reaction between films and substrate becomes significant under thermal treatments for crystallization (Gisser *et al.* 1992, Chen and Wu 1999), ageing (Ishida *et al.* 1996, 1997) and stress relaxation (Zhang and Grummon 1997). This will seriously affect the properties of TiNi shape memory alloys. Therefore, it is important to investigate the interaction of the film–substrate interface at higher temperatures.

Several papers have discussed the interfacial interaction for the Ti or Ni monolayer and Ti/Ni or Ni/Ti bilayers on Si substrates (Horache *et al.* 1989, Setton *et al.* 1989, Sieber *et al.* 1991, Falke *et al.* 1997), but this is indeed different from the TiNi/Si-substrate case. To the best of our knowledge, only two studies have been reported which are related to the TiNi/Si-substrate system (Hung and Mayer 1986, Stemmer *et al.* 1997). Hung and Mayer studied the $Ti_{52}Ni_{48}$ film on Si(100). The $Ti_{52}Ni_{48}$ film crystallizes after 30 min at 450°C and forms a ternary $TiNiSi_2$ compound after 30 min at 625°C (Hung and Mayer 1986). In addition, the interfacial reaction between the Si(100) substrate and nearly equiatomic TiNi film reveals several phases, including a Ti_2Ni compound, a nickel silicide and a ternary titanium nickel silicide (Stemmer *et al.* 1997). Nevertheless, the data are merely available at the 525°C annealing condition and thus could not provide details for the other annealing temperatures.

In this study, near-equiatomic TiNi thin films were rf sputtered on to a Si(100) wafer and then annealed at temperatures between 400 and 700°C for 30 min. The reaction phases and microstructures at the TiNi–Si interface resulting from the post-deposition thermal anneal are investigated. An interfacial evolution mechanism well fitted to the experimental observation is also proposed.

§2. Experimental procedure

Near-equiatomic TiNi thin films were sputtered on to the surface of cleaned and oxide-etched Si(100) wafers, using a rf magnetron gun in an ultrahigh (1×10^{-7} Torr) chamber. The sputtering conditions were as follows: sputtering pressure, 50 mTorr; target–substrate distance, 50 mm; dc power, 200 W; deposition rate, about 5 Å s^{-1}. The target used in this study was a $Ti_{49}Ni_{51}$ disc of 2 inch diameter. The sputter-deposited specimens with thickness of about 1 μm were sealed in evacuated quartz tubes, thermally annealed at 400, 500, 600 and 700°C for 30 min and then furnace cooled to room temperature.

The annealed TiNi films were used to observe the cross-sectional microstructures of the TiNi–Si interface. Cross-sectional transmission electron microscopy (TEM) specimens were fabricated by grinding, dimpling and ion milling at 5 kV to perforation. A sector speed-controlled whisper-lock of a Gatan DuoMill at liquid–N_2 temperature was used to minimize the effects of different ion-milling rates of TiNi and Si in cross-sectional TEM specimens. Microstructure observation was performed using a JEOL model 4000 FX transmission electron microscope operated at 400 kV with 2.6 Å point-to-point resolution and a JEOL field emission transmission electron microscope model 2010F operated at 200 kV with 1.3 Å point-to-point resolution. A dedicated energy-dispersive spectroscopy (EDS) system was employed with both transmission electron microscopes.

§3. Results

3.1. *As-deposited TiNi/Si and specimen annealed at 400°C for 30 min*

The as-deposited TiNi films are amorphous with a columnar structure growing normal on to the Si substrate (Chen and Wu 1999, 2000, Wu *et al.* 2000). The composition of the as-deposited TiNi film is about $Ti_{50.40}Ni_{49.60}$ (in atomic percentages) with a slight fluctuation.

The cross-sectional TEM image of a TiNi/Si specimen annealed at 400°C for 30 min is shown in figure 1 (*a*), and the selected-area diffraction pattern (SADP) of the Si substrate near the interface of figure 1 (*a*), areas C and D, is shown in figure

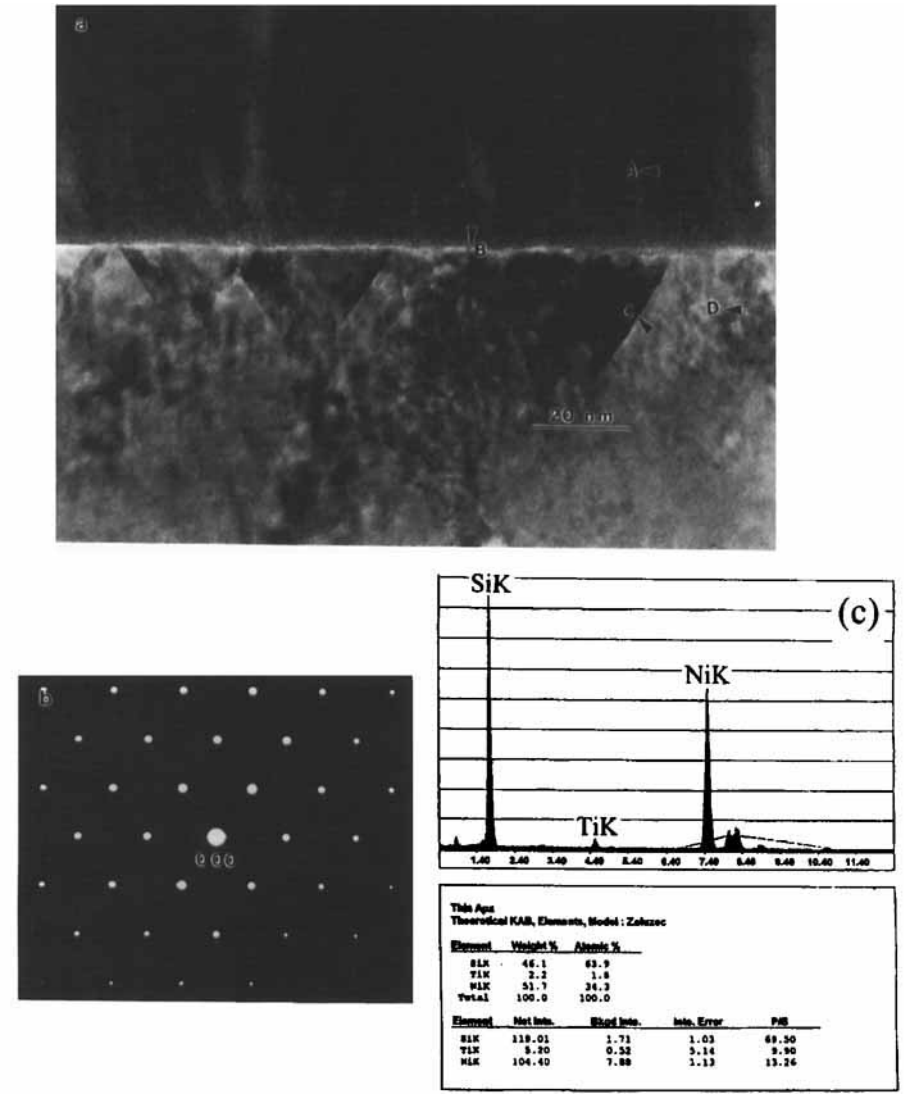

Figure 1. (*a*) The cross-sectional TEM image of a specimen annealed at 400°C for 30 min. Areas A, B, C and D are the TiNi film, (the Si, O)-rich amorphous layer, the triangular $NiSi_2$ and the Si substrate respectively. (*b*) The SADP of the Si substrate. (*c*) The EDS of the triangular C. (*d*) The high-resolution TEM image of the $NiSi_2$–Si interface.

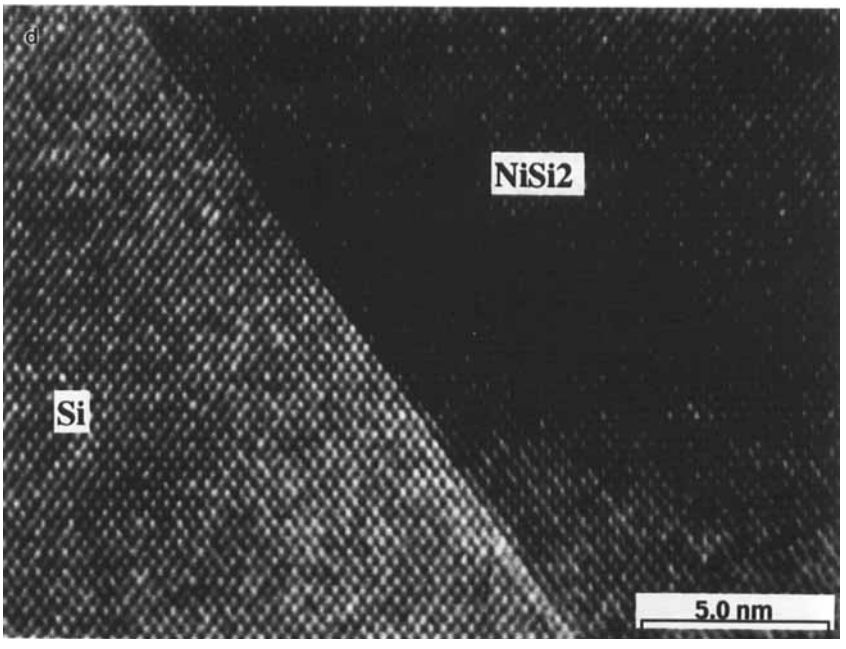

Figure 1. (*continued*)

1 (*b*). The TiNi film in figure 1 (*a*) (area A) is still amorphous. Figure 1 (*c*) is the EDS result of the triangular reaction product (area C) in figure 1 (*a*). Obviously, these triangular products are the $NiSi_2$ compound which has undergone solid solution with a very little Ti.

Figure 1 (*b*) is the SADP of the $\langle 011 \rangle_{Si}$ zone axis. It is also the SADP of the $\langle 011 \rangle_{NiSi_2}$ zone axis. This is due to the epitaxial stress-free growth of $NiSi_2$ on to the Si(100) substrate, as shown in figure 1 (*d*). The lattice constant of Si (diamond structure) is $d = 0.5430$ nm and that of $NiSi_2$ (fcc structure) is $d = 0.5416$ nm. Therefore, the SADPs of $\langle 011 \rangle_{Si}$ and $\langle 011 \rangle_{NiSi_2}$ will coincide with each other owing to very little lattice mismatch (0.25%). The crystal lattice of this disilicide is constructed by replacement involving one Ni atom at (000) and two Si atoms at $(\pm\frac{1}{4} \pm\frac{1}{4} \pm\frac{1}{4})$ (Falke *et al.* 1997). In figure 1 (*a*), the greatest depth of triangular $NiSi_2$ measured from the TiNi–Si interface is about 20 nm. Layer B of figure 1 (*a*) is suggested to be a 2–3 nm (Si, O)-rich layer identified as amorphous (Stemmer *et al.* 1997).

3.2. *Annealing at 500°C for 30 min*

Figure 2 (*a*) shows the cross-sectional TEM image of a TiNi/Si specimen annealed at 500°C for 30 min and figures 2 (*b*) and (*c*) are the SADPs of the silicon substrate and TiNi film near the interface in figure 2 (*a*). As seen in figure 2 (*a*), triangular $NiSi_2$ achieves the greatest depth from the TiNi–Si interface, which is approximately 45 nm. In figure 2 (*a*), most of the epitaxial growth interfaces between $NiSi_2$ and Si are {111} planes, as indicated at A, but occasionally {100} planes can also be observed, as shown at C. Position B in figure 2 (*a*) is the location where perforation can occur most easily during ion milling. Position B is located at the

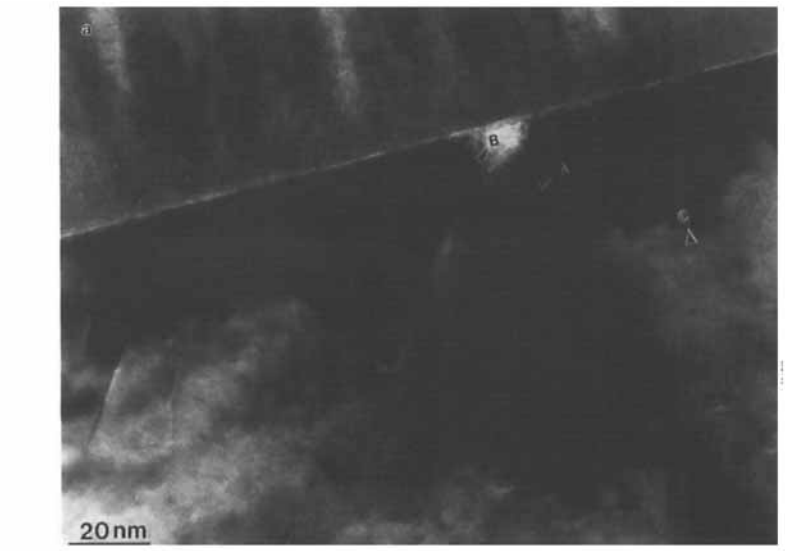

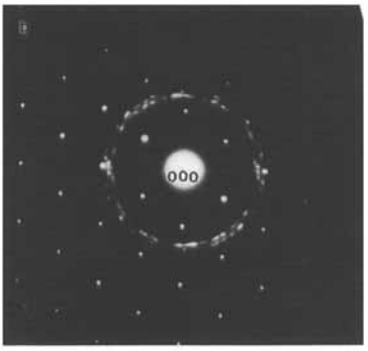

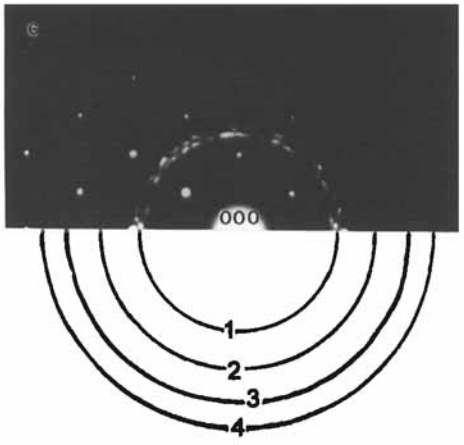

ring	h k l	radius ratio	remark
1	110	$\sqrt{2}$	B2
2	200	$\sqrt{4}$	structure
3	112	$\sqrt{6}$	
4	220	$\sqrt{8}$	

Figure 2. (*a*) The cross-sectional TEM image of a specimen annealed at 500°C for 30 min. Areas B, A and C are a perforation, the {111} plane and the {100} plane of triangular $NiSi_2$ respectively. (*b*) The SADP near the interface. (*c*) Ring patterns. Rings 1–4 correspond to the TiNi B2 phase, but other rings may come from the Ti_2Ni or Ti_2Ni_3Si compounds.

intersection of $NiSi_2$, the Si substrate and the TiNi film, where the largest retained stress may be induced after annealing. In figure 2 (*a*), the amorphous layer 2–3 nm thick still exists.

In figure 2 (*b*), the SADPs of $\langle 011 \rangle_{Si}$ and $\langle 011 \rangle_{NiSi_2}$ are superimposed on the ring pattern of TiNi film near the TiNi–Si interface. The ring pattern in figure 2 (*b*), identified as a B2 structure, is suggested to be the $Ti_{50}Ni_{50}$ B2 austenite phase, as shown in figure 2 (*c*). This ring pattern demonstrates that the amorphous TiNi film just begins to crystallize after 30 min at 500°C. In figure 2 (*b*), the most remarkable ring of TiNi B2 ring pattern is the {011} plane ($d = 0.214$ nm). There are other remarkable rings near the {011} ring of the B2 phase possibly coming from the {511} ring of the Ti_2Ni phase ($d = 0.217$ nm), and/or the (220) ring ($d = 0.21$ nm) or the (115) ring ($d = 0.22$ nm) of the Ti_2Ni_3Si phase (Stemmer *et al.* 1997). As indicated by Stemmer *et al.*, the Ti_2Ni and Ti_2Ni_3Si phases are formed at the TiNi film–Si interface annealed at about 525°C for 30 min.

3.3. *Annealing at 600°C for 30 min*

Figure 3 (*a*) shows the cross-sectional field emission TEM image of a TiNi/Si specimen annealed at 600°C for 30 min. Areas of triangular $NiSi_2$ are still growing and their greatest depth from the TiNi–Si interface approaches 120 nm. Obviously, the (Si, O)-rich amorphous layer is still located between the TiNi film and Si substrate, but its thickness grows from 2–3 nm to about 5 nm at position B. Moreover, no triangular $NiSi_2$ grows from there, implying that the thick amorphous layer may retard the diffusion of Ni atoms from the TiNi film on to the Si substrate. Area D in figure 3 shows the perforation site during ion milling, which is similar to that observed in figure 2 (*a*). However, in figure 3, there are many more perforations and the sizes are larger. This feature may result from the fact that more retained stress exists in the specimen annealed at higher temperatures at the intersection of $NiSi_2$, the Si substrate and TiNi film.

The compositions of positions 1–5 in figure 3 (*b*) are detected using the EDS system of the field emission transmission electron microscope. The EDS data show that positions 1 and 2 have the average composition $Ti_{22.60}Ni_{24.34}Si_{53.06}$, whereas the average composition of positions 3–5 is $Ti_{31.55}Ni_{32.23}Si_{36.22}$. The former is close to the composition of the $Ti_4Ni_4Si_7$ Laves phase and the latter approaches to that of the TiNiSi Laves phase (Settom and Van der Spiegel 1988). Figure 3 shows that the $Ti_4Ni_4Si_7$ compound nucleates between the amorphous layer and $NiSi_2$ and then grows into the triangular $NiSi_2$ and the Si substrate. On the contrary, the TiNiSi compound forms between the amorphous layer and the TiNi film and then grows towards the TiNi film.

3.4. *Annealing at 700°C for 30 min*

Figure 4 (*a*) shows the cross-sectional TEM image of a TiNi/Si specimen annealed at 700°C for 30 min. The compositions of layers A and B, and island C of figure 4 (*a*) have been identified using the EDS system of the transmission electron microscopy, as shown in figure 4 (*b*). Obviously, layer A is TiNiSi, layer B is $Ti_4Ni_4Si_7$ and island C is $NiSi_2$ which has undergone solid solution with several Ti atoms. The thicknesses of layers A and B are more than 0.5 and 0.3 μm respectively. In figure 4 (*a*), $Ti_4Ni_4Si_7$ has now grown to form a layer embedding the triangular $NiSi_2$. The (Si, O)-rich amorphous layer, originally formed at the TiNi–Si interface annealed at a lower temperature, is not present in figure 4 (*a*). This feature may cause

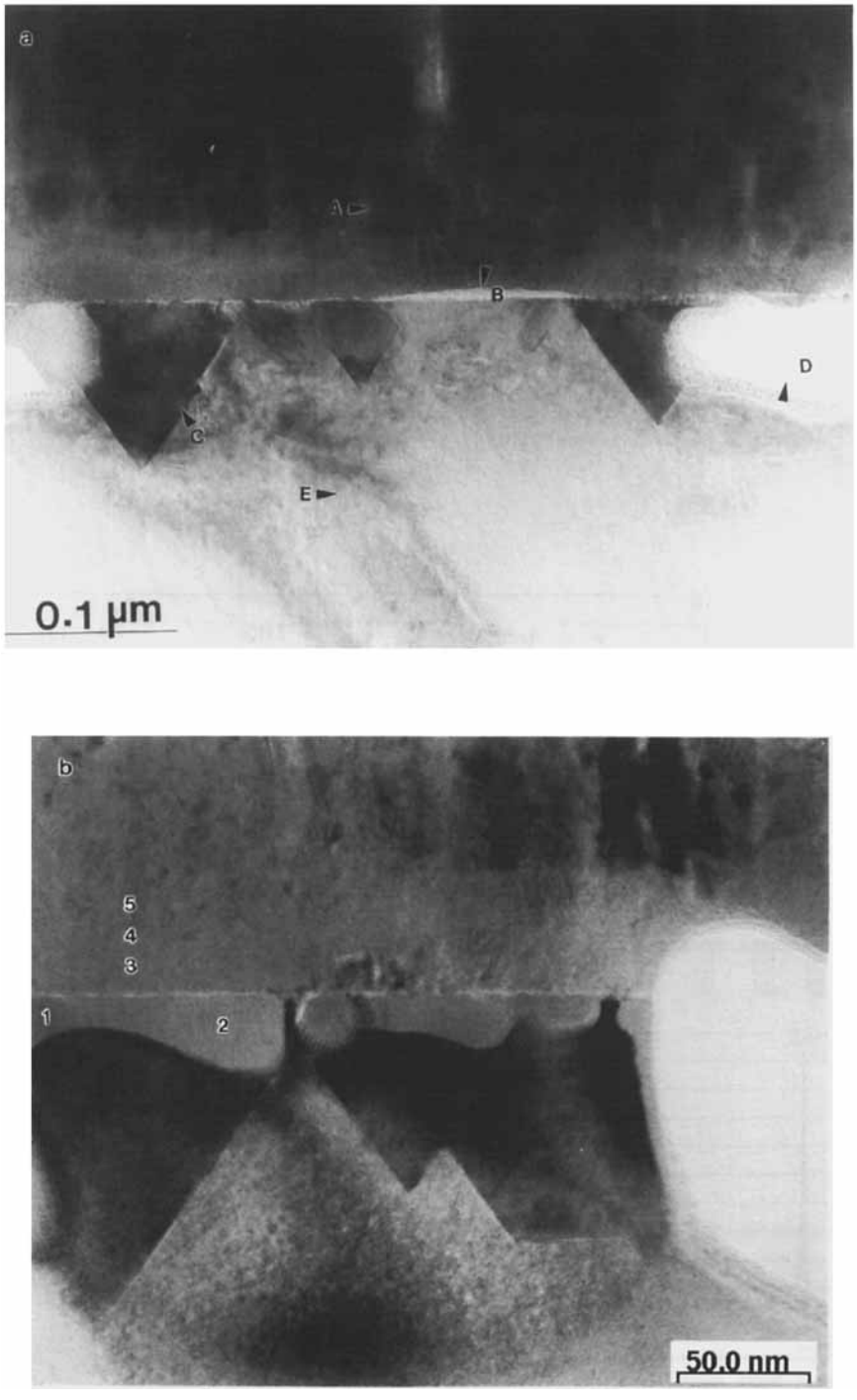

Figure 3. (*a*) The cross-sectional TEM image of a specimen annealed at 600°C for 30 min. Areas A, B, C, D and E are the TiNi film, the (Si, O)-rich amorphous layer, the $NiSi_2$, a perforation and the Si substrate respectively. (*b*) The same as (*a*), but now a phase close to that of the TiNiSi compound forms at positions 3–5 and another phase close to that of the $Ti_4Ni_4Si_7$ compound forms at positions 1 and 2.

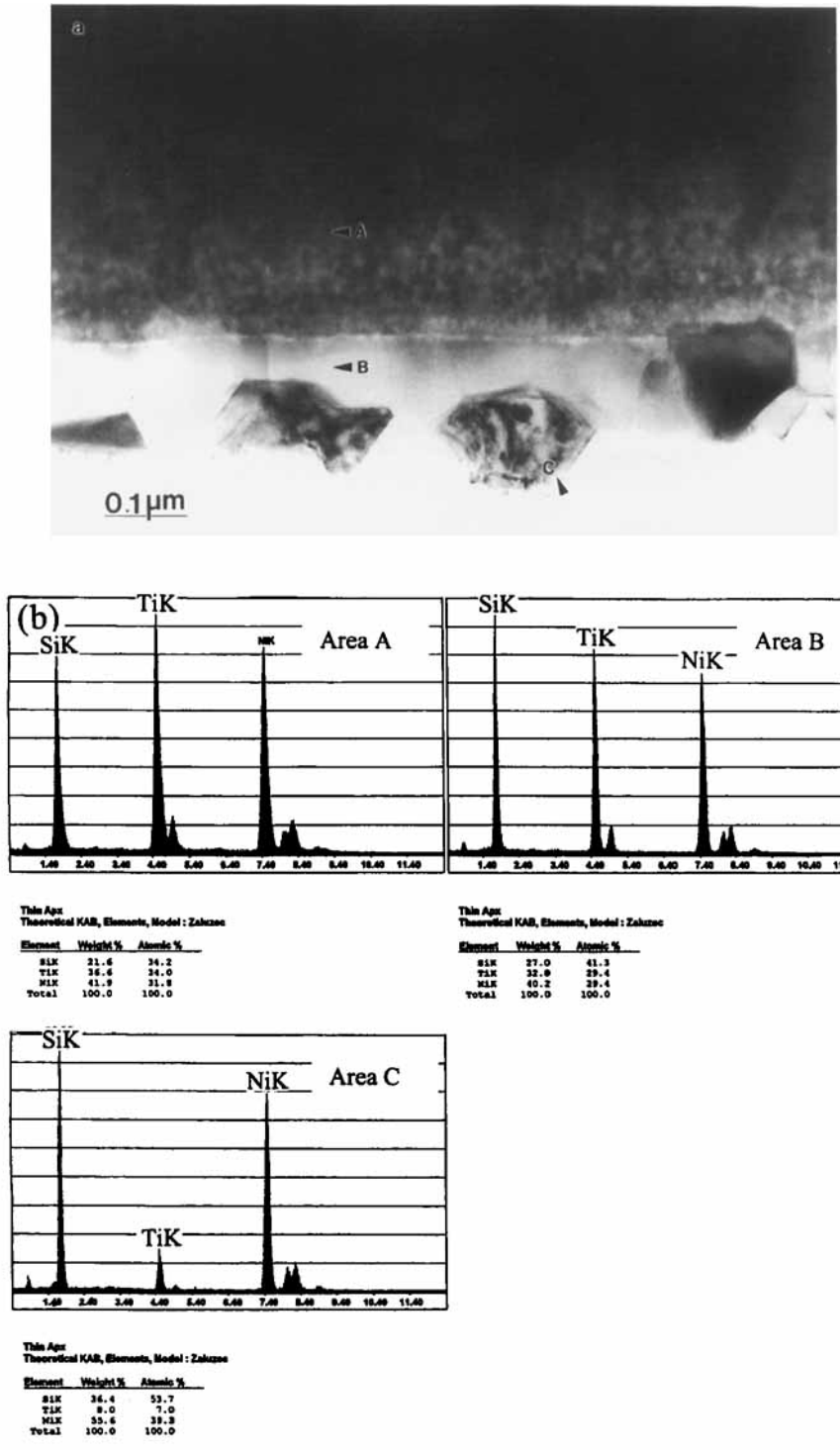

Figure 4. (*a*) The cross-sectional TEM image of a specimen annealed at 700°C for 30 min. Areas A, B and C are TiNiSi, $Ti_4Ni_4Si_7$ and $NiSi_2$ respectively. (*b*) The EDS data of areas A, B and C.

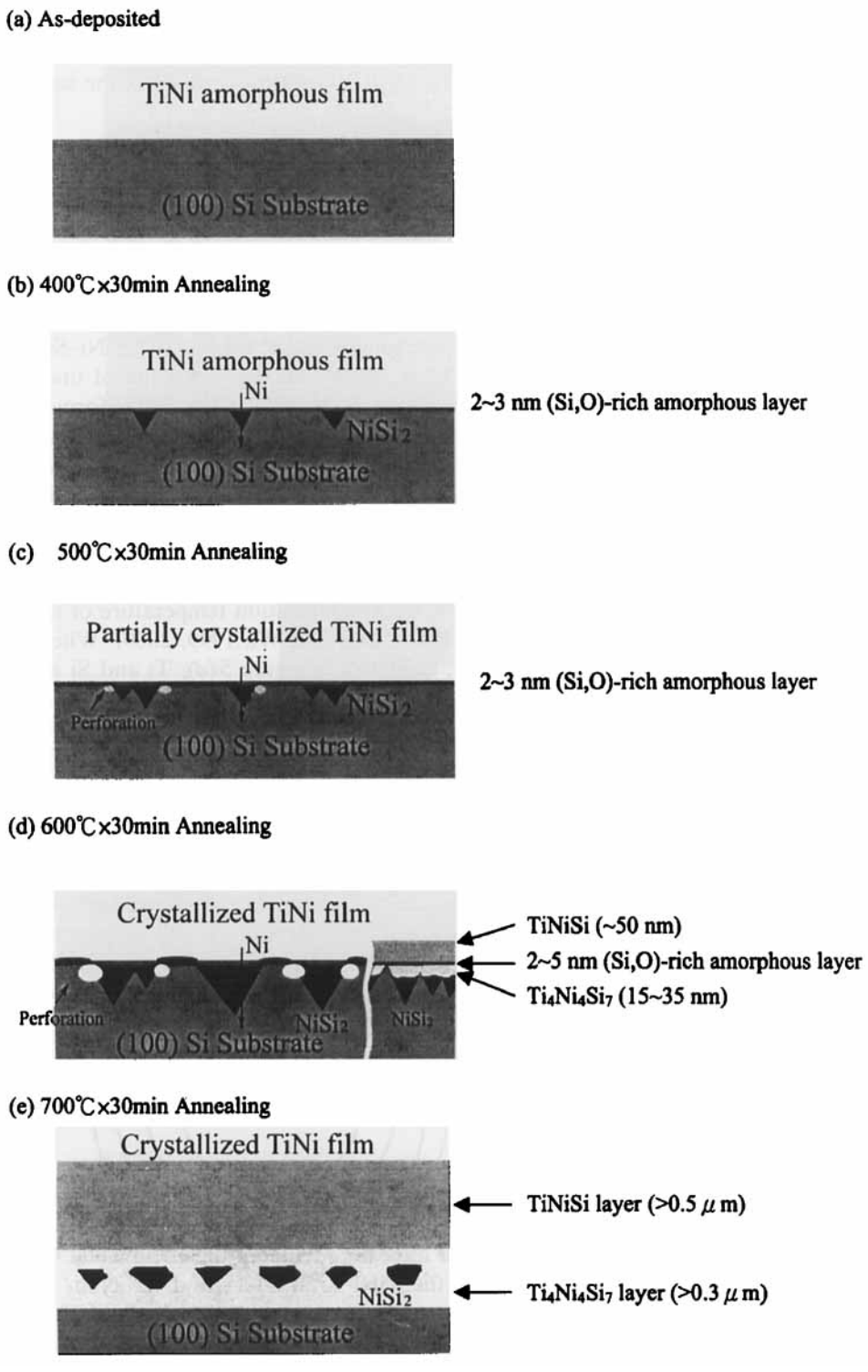

Figure 5. Schematic diagrams of the microstructural evolution of interfacial reaction layers of TiNi/Si annealed at 400–700°C for 30 min.

the Ti and Si atoms to diffuse more quickly. At the same time, the formation of the $Ti_4Ni_4Si_7$ compound in or around triangular $NiSi_2$ may suppress the growth of triangular $NiSi_2$, as the depth of $NiSi_2$ is about 100 nm in figure 4(*a*), the same as in figure 3(*a*).

§4. Discussion

The microstructural evolution of interfacial reaction layers of TiNi film/Si(100) annealed at 400–700°C for 30 min is schematically shown in figure 5. Figure 5(*b*) shows that the triangular $NiSi_2$ begins to grow after 30 min at 400°C from the interface to the Si because the Ni atoms initially migrate from the TiNi film to the Si. The (Si, O)-rich amorphous layer becomes a good diffusion barrier to Ti and Si at low temperatures. This is because the formation of nickel silicide at the Ni–Si-substrate interface is less sensitive to the O-rich layer than the formation of titanium silicide in the Ti/Si-substrate system (Horache *et al.* 1989). The $NiSi_2$ formation, instead of NiSi or Ni_2Si in this study, may be due to the (Si, O)-rich layer which reacts against the diffusion of Ni atoms, leading to a lower Ni supply rate, which facilitates the formation of the Si-rich silicide, $NiSi_2$. According to the Ni–Si phase diagram (Brandes 1983), $NiSi_2$ is the most Si-rich stable intermetallic compound in the Ni–Si system. As the sample is annealed at 500°C for 30 min, as indicated in figure 5(*c*), triangular $NiSi_2$ grows into the Si substrate and the TiNi film begins to crystallize as a $Ti_{50}Ni_{50}$ B2 phase because the crystallization temperature of nearly equiatomic TiNi thin films is around 500°C (Chen and Wu 1999, 2000). When the annealing condition is changed to 600°, as shown in figure 5(*d*), Ti and Si atoms obtain the required energy to penetrate the (Si, O)-rich amorphous layer, and some positions at the TiNi–Si interface reveal ternary Ti–Ni–Si compounds. A near-$Ti_4Ni_4Si_7$ compound nucleates at the interface and grows into the triangular $NiSi_2$ and the Si substrate, and a near-TiNiSi compound also nucleates at the interface and grows into the TiNi film. This means that Si and Ti atoms initially migrate at approximately 600°C. Figure 5(*e*) shows that the $Ti_4Ni_4Si_7$ and TiNiSi ternary compounds have formed two layers between the crystallized TiNi film and the Si substrate. Areas of triangular $NiSi_2$ are embedded in the $Ti_4Ni_4Si_7$ layer and formed isolated islands. The (Si, O)-rich amorphous layer disappears at this interface. The $Ti_4Ni_4Si_7$ is located near the Si substrate because of the abundant Si constituent; on the contrary, TiNiSi grows on the side of the TiNi film owing to the limited Si supply. The diffusion bonding of a bulk thick Si(100) single crystal and bulk $Ti_{50}Ni_{50}$ alloy at 960°C for 6 h also reveals a similar result, that is TiNiSi forms near the $Ti_{50}Ni_{50}$ bulk alloy but $Ti_4Ni_4Si_7$ forms near the bulk Si crystal with the thickness of TiNiSi being much less than that of $Ti_4Ni_4Si_7$ (Wu 1998).

§5. Conclusion

The rf-sputtered TiNi film on Si(100) was annealed at 400–700°C for 30 min and their interfaces are studied using TEM + EDS and field emission TEM + EDS analyses. Experimental results show that, for annealing temperatures below 600°C, Ni atoms are the main species diffusing at the TiNi–Si interface and the $NiSi_2$ compound forms triangularly and grows epitaxially towards the Si substrate. The as-deposited TiNi films are amorphous, but they initially crystallize after 30 min at 500°C. For annealing temperatures higher than 600°C, as well as Ni atoms, Si and Ti atoms also migrate. In certain areas of the TiNi/Si interface annealed at 600°C for 30 min, a ternary compound close to the composition of $Ti_4Ni_4Si_7$ forms into trian-

gular $NiSi_2$ and the Si substrate while a ternary compound close to the composition TiNiSi grows in the TiNi film simultaneously, with the former having a thickness of approximately 15–35 nm and the latter about 50 nm. For the TiNi–Si interface annealed at 700°C for 30 min, the $Ti_4Ni_4Si_7$ compound grows and forms a layer with a thickness of more than 0.3 μm. The $NiSi_2$ compound is now embedded in this layer as isolated islands. The TiNiSi compound also grows and forms a layer of 0.5 μm thickness. A (Si, O)-rich amorphous layer with a thickness of 2–3 nm is also observed in specimens annealed at 400–600°C but disappears in those annealed at 700°C. From the observations of this study, microstructural evolution is proposed to explain the effect of temperature on the formation of interfacial TiNi film–Si(100) reaction layers of annealed at 400–700°C for 30 min.

ACKNOWLEDGEMENTS

The authors are grateful for the financial support of this research from the National Science Council of Taiwan, under grant NSC 88-2216-E002-013.

REFERENCES

BRANDES, E. A. (editor), 1983, *Smithells Metals Reference Book* (London: Butterworth), pp. 11–383.

CHEN, J. Z., and WU, S. K., 1999, *Thin Solid Films*, **339**, 194; 2000, *J. non-crystalline Solids* (submitted)

FALKE, U., FENSKE, F., SCHULZE, S., and HIETSCHOLD, M., 1997, *Phys. Stat. sol.* (a), **162**, 615.

GISSER, K. R. C., BUSCH, J. D., JOHNSON, A. D., and ELLIS, A. B., 1992, *Appl. Phys. Lett.*, **61**, 1632.

HORACHE, E., VAN DER SPIEGEL, J., and FISCHER, J. E., 1989, *Thin Solid Films*, **177**, 263.

HUNG, L. S., and MAYER, J. W., 1986, *J. appl. Phys.*, **60**, 1002.

ISHIDA, A., OGAWA, K., SATO, M., and MIYAZAKI, S., 1997, *Metall. Mater. Trans.* A, **28A**, 1985.

ISHIDA, A., SATO, M., TAKEI, A., NOMURA, K., and MIYAZAKI, S., 1996, *Metall. Mater. Trans.* A, **27**, 3753.

ISHIDA, A., TAKEI, A., and MIYAZAKI, S., 1993, *Thin Solid Films*, **228**, 210.

KRULEVITCH, P., LEE, A. P., RAMSEY, P. B., TREVINO, J. C., HAMILTON, J., and NORTHRUP, M. A., 1996, *J. Microelectromech. Syst.*, **5**, 270.

QUANDT, E., HALENE, C., HOLLECK, H., FEIT, K., KOHL, M., SCHLOßMACHER, P., SKOKAN, A., and SKROBANEK, K. D., 1996, *Sensors Actuators* A, **53**, 434.

SETTON, M., and VAN DER SPIEGEL, J., 1988, *Thin Solid Films*, **156**, 351.

SETTON, M., VAN DER SPIEGEL, J., and ROTHMAN, B., 1989, *J. Mater. Res.*, **4**, 1218.

SIEBER, I., LANGE, H., and SCHADE, K., 1991, *Phys. Stat. sol.* (a), **126**, 171.

STEMMER, S., DUSCHER, G., SCHEU, C., HEUER, A. H., and RUHLE, M., 1997, *J. Mater. Res.*, **12**, 1734.

WALKER, T. A., GABRIEL, K. J., and MEHREGANY, M., 1990, *Sensors. Actuators* A, **21–23**, 243.

WOLF, R. H., and HEUER, A. H., 1995, *J. Microelectromech. Syst.*, **4**, 206.

WU, S. K., CHEN, J. S., and CHEN, J. Z., 2000, *Thin Solid Films*, **365**, 61.

WU, Y. J., 1998, Master's Thesis, National Taiwan University, Taipei, Taiwan.

ZHANG, J., and GRUMMON, D. S., 1997, *Materials for Smart Systems II*, Materials Research Society Symposia Proceedings, Vol. 459, edited by E. P. George (Pittsburgh, Pennsylvania: Materials Research Society), pp. 451–457.